Loading and compressing Cs atoms in a very far-off-resonant light trap

D. J. Han, Marshall T. DePue, and David S. Weiss
Department of Physics, University of California at Berkeley, Berkeley, California 94720-7300
(Received 25 May 2000; published 12 January 2001)

We describe an experiment in which 3×10^7 Cs atoms are loaded into a 400 μm crossed beam far-off-resonant trap (FORT) that is only 2 μK deep. A high-density sample is prepared in a magneto-optic trap, cooled in a three-dimensional far-off-resonant lattice (FORL), optically pumped into the lowest-energy state, adiabatically released from the FORL, magnetically levitated, and transferred to the final trap with a phase-space density of 10^{-3}. Spontaneous emission in the FORT is negligible, and we have compressed the atoms in the FORT to a spatial density of 2×10^{13} atoms/cm^3. Evaporative cooling under these conditions proceeds rapidly.

DOI: 10.1103/PhysRevA.63.023405 PACS number(s): 42.50.Vk, 32.80.Pj

I. INTRODUCTION

Dipole light traps [1] have been used to study cold atom collisions [2,3], to hold atoms during laser cooling [4,5], to evaporatively cool atoms [6], to collect cold molecules [7], and to confine Bose-Einstein condensates (BEC's) in multiple ground states [8]. Ultimately they may be used to trap atoms during precision measurements. All these applications require, to varying degrees, that spontaneous emission due to the trapping light be minimal. They therefore call for the use of far-off-resonant traps (FORT's). Because laser power is limited, FORT's with negligible spontaneous emission must either be small or shallow. The limitations of laser cooling make loading many atoms into such a FORT a technical challenge. We will describe in this paper how we loaded 3×10^7 Cs atoms into a 2 μK-deep, 400-μm crossed dipole trap made from Nd-YAG (yttrium aluminum garnet) laser light [9]. This represents a two order of magnitude increase in the number of atoms that can be loaded into this trap compared to techniques that do not use far-off-resonant optical lattices (FORL's) in the loading process. The techniques we discuss in this paper can also be applied to loading magnetic traps, allowing them to start with phase-space densities exceeding 10^{-3}. Using the known time dependence of evaporation in magnetic traps [10], we infer that such an experiment could reach BEC in seconds, much less than the usual tens of seconds evaporation time scales.

Although having more atoms in the trap can help all the above types of experiments, it is of particular importance in the search for an all-optical approach to BEC, where having many atoms at high phase-space density is central to the task at hand. While evaporative cooling has been demonstrated in a FORT [6] it has not yet produced BEC, largely because heating processes have ultimately outpaced cooling. To be useful for evaporative cooling, a FORT must not cause significant spontaneous emission during evaporation, which will in general take at least 1 s. Since this condition is not met for many traps that are considered FORT's, we will try to avoid confusion in this paper by introducing the term very far-off-resonant trap (VFORT) to describe a FORT that is suitable for evaporative cooling. We demonstrate here that by dynamically compressing our VFORT we can rapidly reach high spatial density. It is hoped in the end that this will speed up evaporative cooling sufficiently that BEC can be reached. While an all-optical approach holds the promise of rapid evaporation for any atomic species, it is of particular importance for Cs, for which it appears that the conventional approach of evaporation in a magnetic trap may not be possible [11–13].

To put as many atoms as possible in a VFORT one wants to maximize the trap volume, the atom density, and the trap depth, while minimizing the temperature of the atoms. But a larger volume trap will usually be a shallower trap, and laser cooling tends to work less efficiently on a large, dense sample. So loading many atoms into a VFORT is a many parameter optimization problem.

The essential features of our experimental solution to this problem are as follows. We first use a transient compression technique in a magneto-optic trap (MOT) in order to maximize the spatial density [14]. We then transfer the atoms to a deep one-dimensional (1D) FORL. After the untrapped atoms have fallen away, we convert the 1D FORL to a 3D FORL, and then laser cool them to near the FORL vibrational ground state using polarization gradient cooling (PGC). We have described PGC at high density in a 3D FORL elsewhere [15,16]. Because FORL-based laser cooling, of which this is but one example [17–21], is so much more effective on dense samples than other laser cooling methods, it is the most important step in our loading procedure.

While the atoms are still in the 3D FORL we optically pump them so that 85% are in the lowest-energy hyperfine sublevel. Because of the tight binding to lattice sites, optical pumping only slightly increases the average vibrational number of the trapped atoms. While they are in the 3D FORL we also turn on an inhomogeneous magnetic field, which is necessary to support them against gravity once they are out of the lattice. When we adiabatically turn off the 3D FORL, there are 4×10^7 atoms at 5×10^{11} atoms/cm^3 with a temperature of 800 nK. They are released into the crossed dipole YAG trap, which captures 73% of them. Once in the VFORT we use a zoom-type optical system to change the size of the trap dynamically.

In the next section we discuss the various options that have been used or proposed for loading VFORT's, in order to put our approach in context. In later sections we present

the details of our experiment, addressing each significant step in the loading in turn.

II. OTHER APPROACHES TO LOADING A VFORT

A. Continuous loading

Since the construction of the first dipole trap [1], the favored way to load them has been to let the atoms continuously fall in from a reservoir of cold atoms, which can be either optical molasses or a MOT. Continuous cooling can then dissipate the energy they pick up falling in, allowing atoms to collect in the trap. For this approach to work, the trap must be deeper than the temperature of the atomic reservoir. If the temperature in the MOT is relatively high, which it will be when the density is high, then the trap depth requirement will seriously limit the VFORT size, and hence the number of atoms trapped. A FORT with sufficiently small detuning can be made deep enough to capture a large fraction of atoms straight from a MOT [22], but then causes enough spontaneous emission that it is not a VFORT. One way to overcome this limitation would be to dynamically change the FORT detuning while evaporatively cooling [22], so that the FORT becomes a VFORT before the temperature is so low that spontaneous emission is unacceptable.

The steady-state number of trapped atoms obtained by continuous loading will occur, of course, when the loading rate equals the loss rate. When the high-density limit is pushed, the maximum density in a MOT is limited by light-assisted collisional loss at the center [23,24,14]. So if the cooling in the VFORT is by the same mechanism as in the MOT, one cannot continuously load the VFORT and achieve a density that is any higher than that in the MOT. The loss rate will be the same in the VFORT and the MOT, but the MOT will not be able to supply atoms to the VFORT any faster than it can supply it's own center.

It may be possible to continuously load a VFORT while using a different cooling mechanism, one that is less likely to result in light-assisted collisions. Any such scheme requires a way to isolate the VFORT from the MOT cooling. This may be accomplished by loading a spatially separated trap [25], but density loss in the transfer process presents a technical challenge. It may also be accomplished in noble gases by allowing atoms to decay into the true ground state, where they can then accumulate [26].

Another possibility is to load a trap whose volume is not directly related to its depth. This is the case with 2D traps with end caps [27,4], and with other types of blue-detuned traps [28]. Atoms can be continuously loaded into a volume that is much larger than the MOT and then compressed. A practical disadvantage of such a technique is that the time scales for making adiabatic changes to a very large trap can be prohibitively long. Blue-detuned traps do have the advantage that the atoms see lower average intensities for the same trap depth, which can make it easier to reach the VFORT regime.

B. Transferring directly from a MOT

Although polarization gradient cooling is effective at the center of a MOT [29], where the magnetic fields are relatively small, the magnetic fields prevent the minimum PGC temperature from being achieved away from the center. Also, the parameters that yield a density maximum do not necessarily coincide with those that yield a temperature minimum. So a VFORT is most efficiently loaded directly from a MOT by first optimizing the density, then turning off the magnetic fields and applying final cooling before the atoms can expand significantly.

For untrapped atoms, the density tends to decrease during cooling as the atoms spatially diffuse. Shelving atoms in a dark state increases the diffusive step size, and makes the density decrease during cooling worse. Still, for large clouds, the effect of the density, n, on the cooling is a more severe problem. Consider the case of polarization gradient cooling. It has been shown that once density dependent heating is appreciable, the temperature at a given intensity and detuning increases as $n^{2/3}N^{1/3}$, where N is the number of atoms [30]. The dependence on density is even more severe when the absolute minimum temperature is desired. Normally for PGC the temperature is proportional to the intensity, but there is a minimum intensity, I_{m}, at which the rms velocity, v_{rms}, of the cooled atoms equals the capture velocity, v_{c}, of the polarization gradient cooling force. For Sisyphus cooling at fixed detuning, $v_{\mathrm{c}} \propto I$. Because PGC is only marginally effective below I_{m}, the velocity distributions become bimodal and the average kinetic energy increases rapidly [31,32]. The density dependence of the temperature shows up in v_{rms},

$$v_{\mathrm{rms}} \propto (In^{2/3}N^{1/3})^{1/2},$$

but not in v_{c}, so I_{m} is density dependent,

$$I_m \propto n^{2/3}N^{1/3}.$$

Therefore the minimum temperature that can be achieved increases as $n^{4/3}N^{2/3}$. For a fixed size atomic cloud, the minimum temperature is proportional to N^2.

Shelving in a dark state can reduce density-dependent heating, but to an extent that is very limited for a heavy atom like Cs. Because the scattering rate has to be small for the lowest temperatures to be reached, and off-resonant excitation to the dark state is infrequent, the atoms must dwell a long time in the dark state if p, the fraction of atoms that are in the hyperfine state that scatters cooling light, is to be kept small. During that time the atoms will fall due to gravity. With relatively low density, we observe a temperature of 3 μK with -20Γ detuning from the $F=4 \rightarrow F'=5$ transition in Cs and an intensity of 1 mW/cm^2, as long as p is kept above 0.4. Figure 1(a) shows a fluorescent image of these atoms after 15 ms of ballistic expansion. If the repumping intensity is lowered so that $p=0.2$, then the average dwell time in the dark is 1 ms. In that time, the atoms pick up 1 cm/s downward velocity, which puts some of them outside of the velocity capture range of PGC when they return to the cooling state. These atoms are not recaptured by PGC, so they lead to a skewed bimodal velocity distribution. Such an unacceptable distribution is shown in Fig. 1(b), which is the same as Fig. 1(a) except that the repumping intensity has been reduced. The dwell time in the dark state can be shortened, while keeping p fixed, by using a combination of

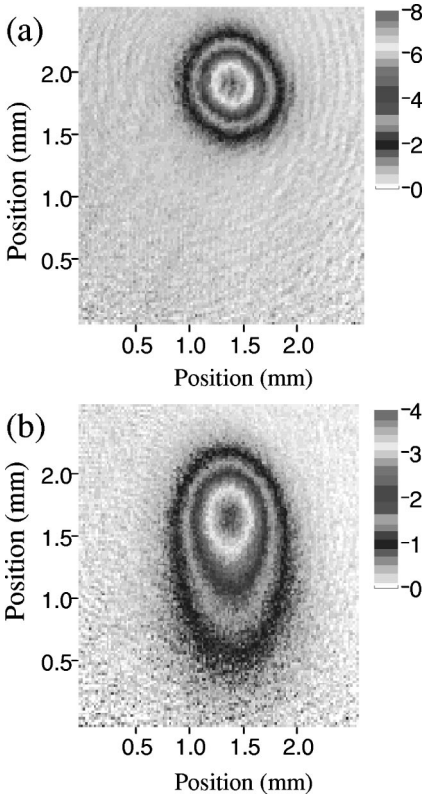

FIG. 1. (a) A fluorescent image after 15-ms ballistic expansion of atoms cooled in free space. The detuning is 20Γ, the intensity is 1 mW/cm^2, and $p=0.4$. (b) The same as (a), but with less repumping intensity, so $p=0.2$. Atoms fall so much when they are in the lower hyperfine level that some are not recaptured by PGC when they return to the cooling transition. (Note that the gray scales of the two pictures are different. To improve contrast, it is not monotonic.)

forced depumping and more repumping; when Townsend *et al.* [23] used forced depumping in a MOT they found that the temperature increased significantly.

For the number and density we achieve in our MOT, we have been unable to cool Cs in free space (i.e., atoms that are not trapped) to a temperature below 10 μK at any detuning or intensity. In contrast, we reach 3μK at low atomic density, and temperatures as low as 1.5 μK have been achieved by PGC with Cs. A higher temperature requires a deeper and therefore smaller VFORT. Since the density cannot be increased, fewer atoms can be loaded into a VFORT when they are hot. A significant increase in the number of atoms loaded into a VFORT requires a new approach to laser cooling, which we have taken using a FORL.

III. PREPARATION IN A 3D FORL

We start our experiment by loading a MOT from a slowed beam of Cs atoms. We then change the MOT parameters in order to achieve a transient density of 1×10^{12} atoms/cm^3 [14]. At the moment when the peak density is reached, we transfer the atoms in place into a 1D FORL, which traps a cylindrically symmetric distribution that is relatively easy to measure. Then we convert the 1D FORL into a 3D FORL, and apply independent light to cool the atoms. Our use of the FORL as an intermediate processing stage increases the number of atoms we load into the VFORT by about two orders of magnitude compared to direct loading techniques.

A. Laser cooling at high density in a FORL

Laser cooling atoms in a 3D FORL with independent cooling light overcomes essentially all of the problems discussed in the previous section. Once atoms are trapped at sufficiently deep 3D FORL sites they no longer collide, so apart from a small (10–15%) transient loss that occurs before all the atoms are bound at sites, the peak MOT density is preserved. Since atoms in a 3D FORL do not fall when they are in a dark state, they can then be cooled at a leisurely pace, while most are shelved in a dark state. By keeping most of the atoms in a dark state, photons are less likely to be rescattered and density-dependent heating is minimized.

We use PGC to cool atoms in the 3D FORL to an average kinetic energy that is comparable to the lattice vibrational frequency, as reported in DePue *et al.* [16]. Coupled with adiabatic release from the lattice this yields a temperature as low as 350 nK for a nonoptically pumped sample. This is half the temperature that has been achieved with low density in a near detuned optical lattice, where the lattice both traps and cools [33]. For this number of atoms at this high of a density, PGC in a FORL yields temperatures that are 30 times lower than what can be achieved by PGC without the FORL.

Similar improvements in temperature can be obtained by Raman sideband cooling in a 3D FORL [20,21]. In fact, PGC in a FORL is conceptually similar to Raman sideband cooling in a FORL, except that PGC does not cool to a vibrational state dependent dark state. Experimentally, we have found that PGC in the 3D FORL can put about 30% of the atoms into the ground vibrational state [16]. This is a better ground-state occupation than is obtained at low density with PGC in a near detuned optical lattice [33], but it is not as good as Raman sideband cooling [20,21]. Also, unlike Raman sideband cooling, PGC does not leave all the atoms in the same internal state, so subsequent optical pumping is needed. But because it is accomplished by just turning the MOT light back on, PGC is experimentally very simple.

Until a method is developed to cool multiple atoms at a site, the density of a laser cooled sample in a 3D FORL (with lattice constants on the order of a visible wavelength) is limited by light-assisted inelastic collisions to about one atom at every other site [16]. Although this is a firmer (and easier to state) limit than for other laser cooling methods, it is less stringent. In fact, even to reach such a high density with a laser cooled sample has, to date, required FORL's [16].

B. Description of the FORL

Our 3D FORL is the superposition of a vertical 1D FORL and a 2D FORL that consists of two orthogonal, horizontal, retroreflected beams (see Fig. 2). All beams are generated from the same Ti-Sapphire laser at 852.739 nm, which is 165 GHz below the $6S_{1/2}$, $F=4\rightarrow6P_{3/2}$ transitions. The particular wavelength is a local minimum for photoassociative

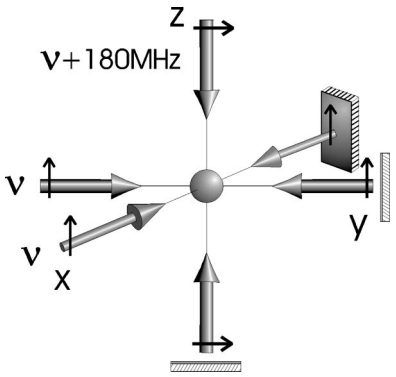

FIG. 2. The FORL beam configuration. Beam polarizations and relative frequencies are indicated.

collisions induced by the FORL light. The empirical choice of this wavelength avoids some loss during the loading, but makes no difference once single atoms are bound to 3D FORL sites. The 1D FORL and the 2D FORL are shifted in frequency with respect to each other by 180 MHz, so that interference between the beams is washed out on longer timescales, like all those related to the cooling and trapping. The 1D FORL is linearly polarized (horizontally) and the 2D FORL is linearly polarized vertically. With no significant interference between the two this makes the net effective polarization in the trap linear. In combination with the large detuning from the upper hyperfine level, this makes the trap nearly identical for atoms in every ground-state hyperfine sublevel [15]. As was reported and discussed in Ref. [15], this is a necessary condition for optimal PGC.

Our 3D lattice intensity has the following analytical form near the center of the beams:

$$I = I_v(\cos kz)^2 + I_h[(\cos ky)^2 + (\cos kx)^2 + 2\cos kx \cos ky \cos \phi], \quad (1)$$

where I_v and I_h correspond to the peak intensities of the vertical and horizontal standing waves, respectively, k is the wave number of the lattice light, and ϕ is the relative phase of the two horizontal standing waves. This relative phase is important to the shape of the potential. When $\phi = \pi/2$ they do not interfere, so the antinodes lie on a square lattice with $\lambda/2$ spacing, as in Fig. 3(a). When $\phi = 0$ they constructively interfere at some antinodes and destructively interfere at others, so that there are half as many potential minima for red-detuned light, each with twice the depth of the antinodes in the out-of-phase case [see Fig. 3(b)]. In the out-of-phase case blue- and red-detuned lattices have identical shapes, but in the in-phase case, blue-detuned light does not trap.

We use an interferometric lock to control the phase of the beams that compose the 2D FORL [34]. Because we need to be able to turn off the FORL completely, and we would like the phase to be correct as soon as it is turned on, we cannot use the Michelson interferometer that is formed by the lattice beams themselves to lock their relative phase. Instead, before the light for the 2D FORL is divided in half, we use a polarizing beam splitter to overlap it with a horizontally polarized beam that is generated from the same laser. The Michelson interferometer output from this beam is always there, and it is separated from the 10 000 times more powerful lattice beams by a slight spatial displacement and two polarizing beam splitters in series. The relative phase of the lattice beams can be monitored independently. The lock beams can be locked at 45 ° relative phase while the lattice beams are at zero relative phase, which obviates the phase dithering usually required for a phase lock at an extremum. We mechanically block the lock beams during most of the time the atoms are in the VFORT.

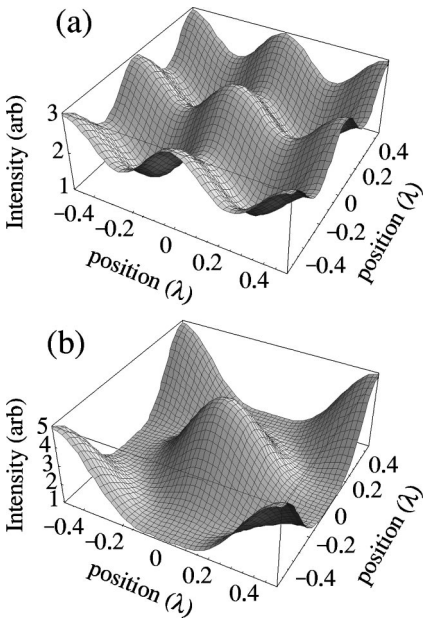

FIG. 3. A horizontal cut of the intensity, and hence the potential, of the 3D optical lattice configured as in Fig. 2. (a) With $\phi = \pi/2$. The potential would look the same if all three standing waves had different frequencies. (b) With $\phi = 0$, I_v, and I_h have both been set equal to 1.

PGC in the FORL is accomplished by the same laser beams that are used for the MOT [15,16]. For optimal cooling we turn off the repump laser completely. Atoms are then only repumped by FORL photons that are spontaneously scattered, a process that occurs at a rate of ~ 200 Hz per atom. At any given time 97% of the atoms are stored in the lower hyperfine level during cooling. An intensity of 7.5 mW/cm^2 leads to a 3D ground-state occupation of 0.3.

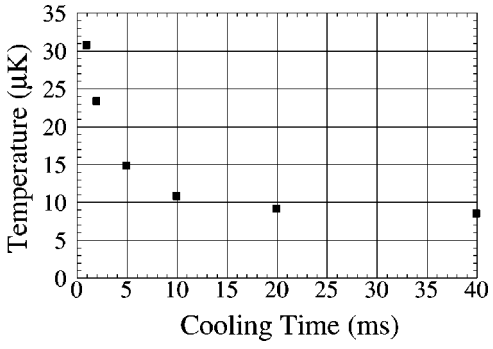

FIG. 4. The time dependence of PGC in the 3D FORL. The conditions are close to those that yield the lowest temperature. The steady-state fraction of atoms in the upper hyperfine level is 0.08.

As illustrated in Fig. 4, the cooling is complete after 20 ms. Because of the isolation of atoms at the center of 3D FORL sites, atom loss during the cooling is negligible.

IV. OPTICAL PUMPING AND LEVITATION

A. General considerations

To reach high phase space density by evaporative cooling, all the atoms must be in the same internal state. A spin-aligned sample is also necessary in order to levitate heavy atoms in a large shallow trap. Single state occupancy can be achieved by either state selection or optical pumping, but because the ground state is so highly degenerate in Cs, optical pumping is much preferred. With many atoms at high density the reabsorption of scattered photons can be a big problem for optical pumping, making it a slow process with a lot of heating. As with density-dependent problems in laser cooling, trapping in the 3D FORL largely overcomes these density-dependent optical pumping problems.

There are three benefits to optical pumping in the lattice. First, just as the cooling rate in the 3D FORL was unimportant, nothing is lost if optical pumping in a 3D FORL takes a long time. Second, the heating rate in an optical lattice can also be reduced compared to that in free space. This reduction was first observed in Winoto *et al.* [15], and is studied in detail in Ref. [35].

The third and probably most important advantage to optical pumping in the 3D FORL is that the same amount of heating has less of an effect on the final free space temperature. Ignoring density-dependent effects, the change in energy on average when a photon is scattered is the same in and out of the lattice. Deep in the Lamb-Dicke regime most of the scattered photons cause no recoil heating, but those that do, give a random energy change of $\hbar\omega$, which is much larger than a photon recoil energy [36]. But adiabatic release from the FORL decreases this differential increase in energy just as it decreases the total energy. For example, scattering an average of 20 photons will increase the energy of an ensemble of Cs atoms by K_B 4 μK. Atoms in a lattice with k_B 8μK level spacing and an initial average kinetic energy of k_B 10 μK will have a temperature of 0.5 μK after adiabatic release. After scattering those 20 photons they will only be 0.4 μK hotter after adiabatic release, an 80% increase in final temperature. In contrast, optical pumping would increase the temperature of an initially 0.5 μK sample of atoms in free space by a factor of 9.

In order to load our shallow, large VFORT it is necessary to levitate the atoms. The gravitational potential energy of Cs at a height of 0.4 mm (the initial trap waist size) is 63 μK, which dwarves the initial trap depth of 2.5 μK. Without levitation there would be no trap. We generate the levitating field with the same anti-Helmholtz coils that are used for the MOT. By varying the relative current in the two sets of coils, while keeping the sum of the currents constant, we can vary the magnetic bias field while maintaining levitation. Eddy currents induced in our vacuum chamber require 20 ms to fully die out. If the 3D FORL were on during this time, residual spontaneous scattering could compromise the optical pumping. Accordingly, we turn the bias field on while the atoms are still in the 3D FORL, and perform the optical pumping discussed below in bias fields greater than 20 G. We shut off the FORL adiabatically immediately after the optical pumping.

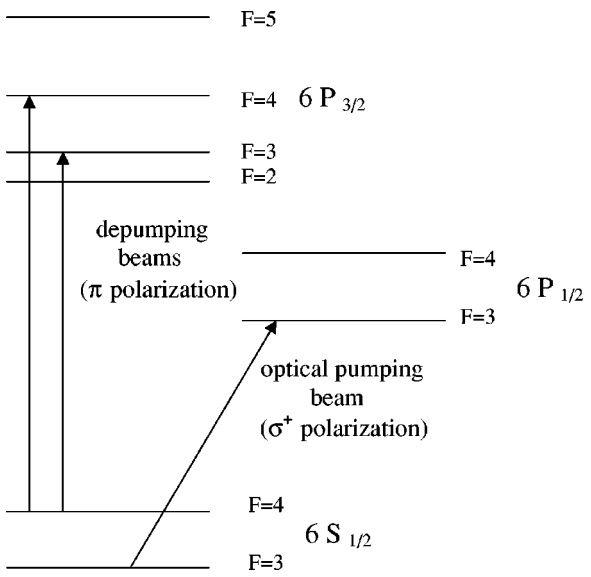

FIG. 5. Optical pumping diagram. The depumping beams propagate horizontally and the optical pumping beam propagates exactly along the vertical axis. Energies on the vertical axis are not to scale.

B. Experimental results

We optically pump to the lowest energy $F=3$, $m_F=3$ state using three traveling-wave optical pumping beams (see Fig. 5). One is circularly polarized along the vertically oriented bias field, copropagating with the vertical lattice beams, and resonant with the (zero B field) $6S_{1/2}$, $F=3 \rightarrow 6P_{1/2}$, $F'=3$ transition. The other two are linearly polarized vertically, copropagate horizontally, and are near resonant with the $6S_{1/2}$, $F=4 \rightarrow 6P_{3/2}$, $F'=3$ and $6S_{1/2}$, $F=4 \rightarrow 6P_{3/2}$, $F'=4$ transitions, respectively. The beams have 100 mW/cm^2.

We monitor the optical pumping by releasing the atoms into free space, and observing the number of levitated atoms compared to the total number of atoms. At the same time we can do a ballistic temperature measurement of the levitated atoms, in order to measure the heating caused by optical pumping. Figure 6 shows fluorescent pictures of the atoms 40 ms after being released into the gradient magnetic field. In Fig. 6(a), where there has been no optical pumping, atoms are visible in (from top to bottom) the F, m_F levels: 4, -4; 3, 3, and 4, -3; and 3, 2 and 4, -2. After optical pumping, as in Fig. 6(b), 95% of the atoms are in the 3, 3 sublevel.

Optical pumping takes several milliseconds, and causes only modest heating compared to the average energy of the FORL-trapped atoms. The number of atoms in the $F=3$, $m_F=3$ sublevel and the temperature, measured after a totally nonadiabatic release from the FORL, are plotted in Fig. 7 as a function of time.

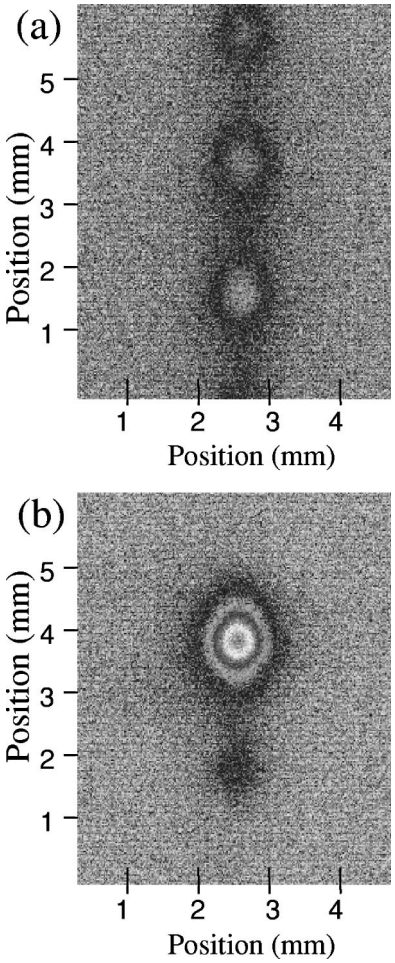

FIG. 6. Stern-Gerlach picture of the atoms. (a) A nonoptically pumped sample. From top to bottom, the clouds contain atoms in: $|F=4,\ m_F=-4>$; $|F=3,\ m_F=+3>$, and $|F=4,\ m_F=-3>$; $|F=3,\ m_F=+2>$, and $|F=4,\ m_F=-2>$. (b) An optically pumped sample. Analysis of the picture shows that 95% of the atoms are spin polarized to the $|F=3,\ m_F=+3>$ state. (The gray scale is the same for both pictures. To improve contrast, it is not monotonic.)

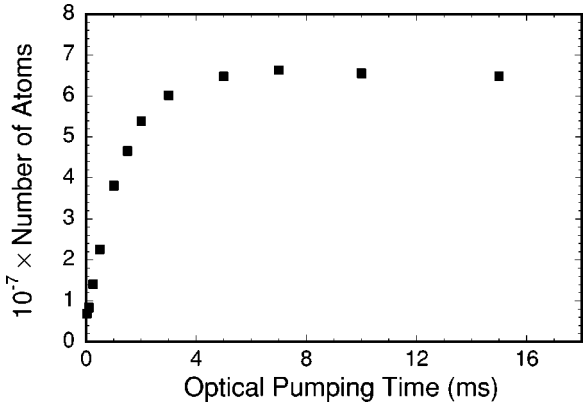

FIG. 7. Number of atoms that are optically pumped into the $|F=3,\ m_F=+3>$ state as a function of the optical pumping time. The data is obtained from pictures like that shown in Fig. 6(b).

V. LOADING THE CROSSED DIPOLE TRAP

A. General considerations

Adiabatic release from the 3D FORL is accomplished by reducing the light intensity according to $I(t)=I_0(1+At)^{-2}$, which maintains the same degree of adiabaticity throughout [33]. We determine the time constant A empirically, to minimize the final temperature. We smoothly shut off the FORL in all directions by a factor of 1000, using an acousto-optic modulator. An rf switch in the driver completes the shutoff.

Figure 8 shows the final temperature after a 1D FORL is shut off with different exponential time constants, starting from a relatively high initial temperature. It serves to illustrate the central features of our 3D FORL adiabatic shutoff. The transition from fully nonadiabatic to adiabatic is clearly visible, as is the fact that adiabatic cooling is insensitive to the time constant as long as it is sufficiently slow.

The VFORT consists of two crossed, horizontal traveling waves, generated from the same YAG laser with 1.064 μm wavelength. Such a trap was first demonstrated in Ref. [6]. The beams are identical except that one is linearly polarized horizontally and the other vertically. They are focused to 20-μm spots, but at the point where the two beams intersect their waists are 400 μm. The power in each traveling wave is 2.7 W, so that the peak ac Stark shift experienced by the atoms is $U_{\rm ac}=k_B\times(5\ \mu{\rm K})$.

The orthogonality of the beam polarizations ensures that there is no intensity standing wave. There is a periodic variation in the trap polarization, but this does not translate into a periodic change in the trap potential as long as the atoms are trapped in a single Zeeman sublevel defined by a quantization axis oriented along one of the beam polarization directions. In this case the Stark shift everywhere is equal to that due to linearly polarized light. One could also avoid any interference between the crossed beams by frequency shifting one of them, as we do in our 3D FORL. It is necessary that the magnetic bias field be much greater than the ac Stark shift due to the trap so that stimulated Raman transitions

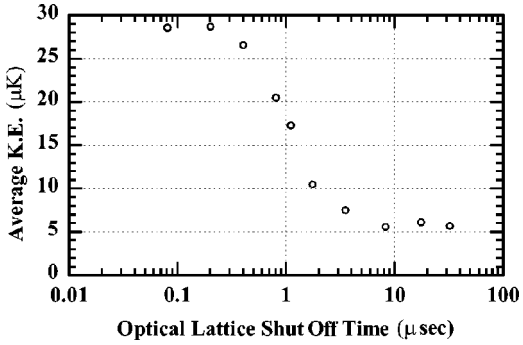

FIG. 8. Adiabatic release from a 1D FORL. The temperature of the atoms in the confining direction is shown as function of time constant with which the FORL is shut off. The essential behavior of the adiabatic release is illustrated here. For loading our crossed dipole trap, we use a 3D FORL, and start and end with much lower temperatures.

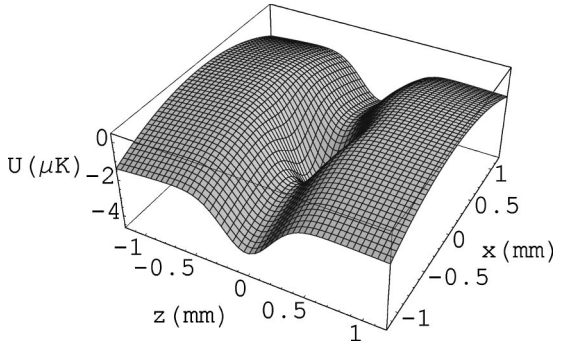

FIG. 9. The crossed dipole trap potential (in the presence of a levitating magnetic field). The *z* direction is vertical, perpendicular to both dipole beams, while the *x* direction is along one of the beams.

cannot remove atoms from the lowest-energy state.

Because the atoms are trapped in the strong field seeking magnetic sublevel, the levitation plus bias field constitutes a magnetic antitrap. This serves the useful purpose of providing a well-defined 3D ledge around the trap, but it also decreases the trap depth in all directions. Combining the effects of the VFORT and the antitrap, the horizontal and vertical trap depths are 1.2 and 4.9 μK, respectively, when the trap bias field is 20 G, and 1.8 and 4.9 μK when the trap bias field is 50 G. An *x*-*z* cross-section of the trap potential is shown in Fig. 9.

B. Experimental results

Measuring the trap loading efficiency is somewhat complicated by the evaporative cooling that occurs from the outset. With the levitating magnetic field on, atoms in the trap region, but outside the trap, take a significant amount of time to leave ballistically. The background of atoms, particularly those in the nonintersecting parts of the YAG beams, is much easier to interpret after a couple of hundred milliseconds. Accordingly we measure the number of atoms in the trap 500 ms after the FORL is shutoff adiabatically, and infer the initial trap number from the loss rate at that time. The number of trapped atoms as a function of the trap size, at constant YAG power, is shown in Fig. 10. There is a clearly optimal size, which is a trade off between the trap size limiting the fraction of atoms captured, and the trap being too shallow. At the peak, 3×10^7 atoms are initially trapped, which corresponds to 70% of the FORL-cooled atoms.

VI. COMPRESSION IN THE CROSSED DIPOLE TRAP

After many atoms are loaded into the VFORT it is often desirable to compress them. Adiabatic compression increases the spatial density at no cost to the phase-space density. It also increases the trap oscillation frequency, which is particularly important in the hydrodynamic limit [37,19], where the evaporation rate is limited by the trap oscillation frequency. Compression is executed by a zoom lens system.

Compression should proceed slowly enough to avoid significant nonadiabatic heating. In the hydrodynamic limit, the relevant time scale is the horizontal trap oscillation frequency, ω_h, because that is the thermal equilibration time. The trap oscillation frequency is proportional to P/w^2, where w is the beam waist at intersection and P is the power in the dipole beams. We can define a dimensionless parameter $X=\omega^{-2}d\omega/dt$, to characterize the extent to which a change in the trap is adiabatic. When $X\ll1$, changes are adiabatic. If we ignore evaporation from the trap, then the ratio of temperature to trap depth, which we call Q, does not change when w is reduced while P is kept constant. It is possible to keep X constant during compression at fixed power by reducing the waist according to the equation $w=w_0\sqrt{1-t/\tau}$, where τ is a time constant.

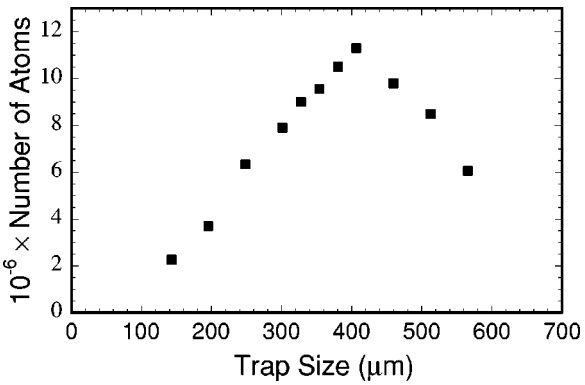

FIG. 10. Number of atoms loaded into the YAG trap at different trapping beam sizes (e^{-2} radius). The data are taken 500 ms after the atoms are loaded. The best mode matching occurs when the trap is 400 μm, where 70% of the atoms are captured.

Evaporation can be forced by lowering P, and hence Q. Then there are many alternative strategies, but a notable one is one in which the evaporation per cycle, $Y=\omega^{-1}dQ/dt$, is kept constant. This can be accomplished when $w=w_0\ \exp(-t/\tau)$ and $P=P_0\ \exp(-2t/\tau)$. In this strategy, X decreases exponentially.

A. Experimental setup

Our zoom lens configuration is shown in Fig. 11. The beam is nearly collimated between lens 2 and lenses 3 and 4, so that the exact distance between them is not critical. Lens 2

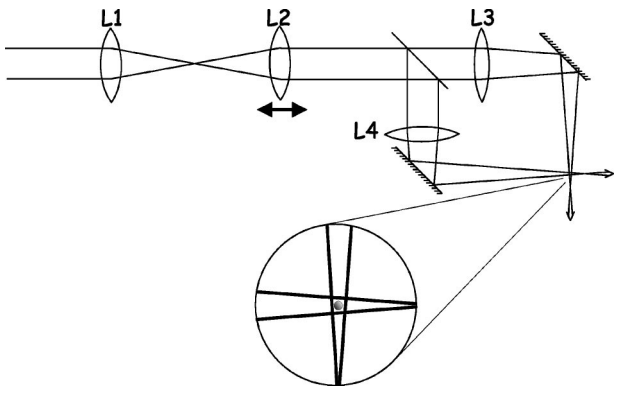

FIG. 11. The zoom lens configuration for YAG trap compression. The lens L2 is moved by a precision translation stage in order to change the beam radii at their point of intersection.

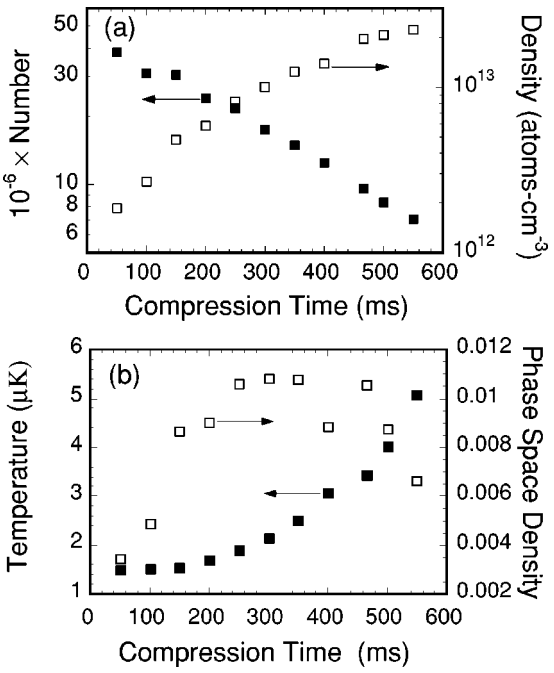

FIG. 12. Evolution of the trapped atoms during compression. (a) Number and density as functions of compression time. (b) Temperature and phase-space density as functions of compression time. The solid squares refer to number and temperature, which are the directly measured quantities here. The trap waist is decreased exponentially with a time constant of 500 ms. Because the trap power is fixed, evaporation is not forced during this compression.

is translated by a computer controlled Newport Model MM3000 stage. The translation is executed so that the beam waist at the trap intersection point varies in a well-defined way, usually exponentially. The motion produces the most nonadiabatic changes in the trap when the stage is accelerated initially and when its motion is finally stopped. When we double the acceleration of the stage at these times, but otherwise keep its motion the same, we do not see a significant change in atom temperature and number. We thus infer that the heating due to translation stage motion is negligible during our compression. A 3.4-mm lens translation changes the location of the dipole trap focus by 14 mm, which changes the trap size from 400 μm to 50 μm.

B. Results

We have compressed without forcing evaporation by decreasing the waist exponentially in time. In Fig. 12 we plot the temperature, number, density, and phase-space density of atoms in the trap as a function of compression time, using a compression time constant of 500 ms. Temperature and number are directly measured, while density and phase-space density are derived assuming that the trap is harmonic [38], which is a reasonably good approximation. Unforced evaporation occurs during compression, so that in the first 250 ms the phase-space density increases by a factor of 5. After 560 ms, when the trap beam radii at the point of intersection is 130 μm, losses have outpaced evaporation, and the phase-space density has started to fall. With that beam size, trapped atoms spontaneously emit YAG photons at a rate of 0.3 Hz, so the trap intensity should be reduced if the trap is compressed to such a degree.

We have also forced evaporation by lowering the trap depth, both during and after compression. To date, we have reached to within a factor of 10 of quantum degeneracy, but eventually heating outpaces evaporation. The heating does not appear to depend on the YAG intensity. We are in the process of studying the heating, which combined with evaporation, presents itself predominantly as a density-independent loss. Among the heating mechanisms that have been discussed in the literature are grazing collisions with the background gas [39], trap intensity fluctuations and beam pointing instability [40,41], and photoassociative collisions [3]. Our calculations and observations suggest that none of these mechanisms is severe enough to prevent condensation. Alternative approaches to evaporation are possible and might make it easier to diagnose unwanted heating. For our trap configuration in particular, microwave evaporation, using the levitation field to discriminate among the atoms, holds some promise. Further discussion of forced evaporation is beyond the scope of this paper.

VII. CONCLUSIONS

A. Summary

We have described an experiment to load 3×10^7 atoms into a VFORT, a trap with negligible spontaneous emission on evaporative cooling timescales. In the first experimental stage, a Cs density of 1×10^{12} atoms/cm^3 with 3×10^8 atoms is obtained by dynamically compressing a large MOT [14]. Atoms at the MOT center are then transferred in place into a 1D FORL and then a 3D FORL. Our implementation of a 3D FORL is ideal for PGC, which cools 30% of the atoms into the 3D vibrational ground state. After cooling, the atoms are optically pumped into the lowest-energy state, defined by a magnetic field that also has a gradient sufficient to levitate atoms in this state. The atoms pick up 4 μK of energy during the optical pumping, but this represents only modest heating after the atoms are adiabatically released from the FORL.

We adiabatically release the atoms into a crossed dipole YAG trap, 2-μK deep with a 400-μm waist. Upon loading, the atoms have a phase-space density of 10^{-3} and are already in the hydrodynamic limit of motion in the trap. The volume of the trap can then be compressed by as much as a factor of 1000.

B. Discussion

There is room to improve the initial phase-space density and number in the trap. Incorporating FORL-based compression can increase the initial spatial density by a factor of 6, with little temperature change, but at the cost of up to a factor of 2.5 in atoms [16]. Compression techniques can also help to match the FORL-trapped cloud in shape to that of the VFORT.

Raman cooling in 3D can be implemented to cool the atoms to perhaps as low as 100 nK after adiabatic shutoff,

with most of them in the lowest-energy state. It is difficult but probably not impossible to translate lower temperatures into a better initial trap condition, because a low temperature must have a comparably shallow VFORT, which will have an extremely low initial oscillation frequency. Compression must therefore be very slow in order to be adiabatic, and background losses from the trap can start to dominate.

Higher numbers of atoms can be trapped using the same basic techniques if the FORL is enlarged. If at the same time the FORL beams were brought closer to resonance this could be done without even sacrificing depth. A doubling of the FORL size, and possibly mode matching to the MOT's asymmetry, could allow for more than 10^9 atoms to be processed in this way. Density-dependent effects might become important before that point, but one of the essential features of FORL-based laser cooling is that it is very insensitive to atom density and number.

ACKNOWLEDGMENTS

We acknowledge useful discussions with Steven Oliver and Lukman Winoto, as well as their technical assistance. We thank the Office of Naval Research, the National Science Foundation, and the Packard Foundation for supporting this work.

[1] S. Chu, J. E. Bjorkholm, A. Ashkin, and A. Cable, Phys. Rev. Lett. **57**, 314 (1998).
[2] J. D. Miller, R. A. Cline, and D. J. Heinzen, Phys. Rev. Lett. **71**, 2204 (1993).
[3] A. Fioretti, D. Comparat, A. Crubellier, O. Dulieu, F. Masnou-Seeuws, and P. Pillet, Phys. Rev. Lett. **80**, 4402 (1998).
[4] H. J. Lee, C. S. Adams, M. Kasevich, and S. Chu, Phys. Rev. Lett. **76**, 2658 (1996).
[5] H. Perrin, A. Kuhn, I. Bouchoule, T. Pfau, and C. Salomon, Europhys. Lett. **46**, 141 (1999).
[6] C. S. Adams, H. J. Lee, N. Davidson, M. Kasevich, and S. Chu, Phys. Rev. Lett. **74**, 3577 (1995).
[7] T. Takekoshi, B. M. Patterson, and R. J. Knize, Phys. Rev. Lett. **81**, 5105 (1998).
[8] D. M. Stamper-Kurn, M. R. Andrews, A. P. Chikkatur, S. Inouye, H.-J. Miesner, J. Stenger, and W. Ketterle, Phys. Rev. Lett. **80**, 2027 (1998).
[9] M. T. DePue, D. J. Han, C. McCormick, S. L. Winoto, S. Oliver, and D. S. Weiss, BAPS, Centennial Meeting, OB16.12, 1999.
[10] B. P. Anderson and M. A. Kasevich, Phys. Rev. A **59**, R938 (1999).
[11] J. Söding, D. Guery-Odérlin, P. Desbiolles, G. Ferrari, and J. Dalibard, Phys. Rev. Lett. **80**, 1869 (1998).
[12] D. Guery-Odèrlin, J. Söding, P. Desbiolles, and J. Dalibard, Opt. Express **2**, 323 (1998).
[13] S. J. J. M. F. Kokkelmans, B. J. Verhaar, and K. Gibble, Phys. Rev. Lett. **81**, 951 (1998).
[14] M. T. DePue, S. L. Winoto, D. J. Han, and D. S. Weiss, Opt. Commun. **180**, 73 (2000).
[15] S. L. Winoto, M. T. DePue, N. E. Bramall, and D. S. Weiss, Phys. Rev. A **59**, R19 (1999).
[16] M. T. DePue, C. McCormick, S. L. Winoto, S. Oliver, and D. S. Weiss, Phys. Rev. Lett. **82**, 2262 (1999).
[17] S. E. Hamann, D. L. Haycock, G. Klose, P. H. Pax, I. H. Deutsch, and P. S. Jessen, Phys. Rev. Lett. **80**, 4149 (1998).
[18] H. Perrin, A. Kuhn, I. Bouchoule, and C. Salomon, Europhys. Lett. **42**, 395 (1998).
[19] V. Vuletic, C. Chin, A. Kerman, and S. Chu, Phys. Rev. Lett. **81**, 5768 (1998).
[20] A. J. Kerman, V. Vuletić, C. Chin, and S. Chu, Phys. Rev. Lett. **84**, 439 (2000).
[21] D. J. Han, S. Wolf, S. J. Oliver, C. McCormick, M. T. DePue, and D. S. Weiss, Phys. Rev. Lett. **85**, 724 (2000).
[22] K. Corwin, S. Kuppens, D. Cho, and C. Wieman, Phys. Rev. Lett. **83**, 1311 (1999).
[23] C. G. Towsend, N. H. Edwards, K. P. Zetie, C. J. Cooper, J. Rink, and C. J. Foot, Phys. Rev. A **53**, 1702 (1996).
[24] H. Katori, T. Ido, and M. Kuwata-Gonokami, J. Phys. Soc. Jpn. **68**, 2479 (1999).
[25] M. Hammes, D. Rychtarik, V. Druzhinina, U. Moslener, I. Manek-Honninger, and R. Grimm, http://xxx.sissa.it/abs/physics/0005035 (2000).
[26] H. Gauck, M. Harti, D. Schneble, H. Schnitzler, T. Pfau, and J. Mlynek, Phys. Rev. Lett. **81**, 5298 (1998).
[27] T. Kuga, Yoshio Torii, N. Shiokawa, T. Hirano, Y. Shimizu, and H. Sasada, Phys. Rev. Lett. **78**, 4713 (1997).
[28] N. Friedman, L. Khaykovich, R. Ozeri, and N. Davidson, Phys. Rev. A **61**, 031 403 (2000).
[29] A. M. Steane and C. J. Foot, Europhys. Lett. **14**, 231 (1991).
[30] C. J. Cooper, G. Hillenbrand, J. Rink, C. G. Townsend, K. Zetie, and C. J. Foot, Europhys. Lett. **28**, 397 (1994).
[31] J. Dalibard and C. Cohen-Tannoudji, J. Opt. Soc. Am. B **6**, 2023 (1989).
[32] D. S. Weiss, E. Riis, Y. Shevy, P. J. Ungar, and S. Chu, J. Opt. Soc. Am. B **6**, 2072 (1989).
[33] A. Kastberg, W. D. Phillips, S. L. Rolston, R. J. C. Spreeuw, and P. S. Jessen, Phys. Rev. Lett. **74**, 2253 (1995).
[34] A. Hemmerich, C. Zimmermann, and T. W. Hänsch, Phys. Rev. Lett. **72**, 625 (1994).
[35] S. Wolf, S. J. Oliver, and D. S. Weiss, Phys. Rev. Lett. **85**, 4249 (2000).
[36] D. Wineland and W. Itano, Phys. Rev. A **20**, 1521 (1999).
[37] Yu Kagan, E. L. Surkov, and G. V. Shlyyapnikov, Phys. Rev. A **55**, R18 (1997).
[38] D. J. Han, University of Texas at Austin, Ph.D. thesis, 1998.
[39] S. Bali, K. M. O'Hara, M. E. Gehm, S. R. Granade, and J. E. Thomas, Phys. Rev. A **60**, R29 (1999).
[40] T. A. Savard, K. M. O'Hara, and J. E. Thomas, Phys. Rev. A **56**, R1095 (1997).
[41] M. E. Gehm, K. M. O'Hara, T. A. Savard, and J. E. Thomas, Phys. Rev. A **58**, 3914 (1998).